

A Structure for Quasars

Martin Elvis

Harvard-Smithsonian Center for Astrophysics, Cambridge MA 02138, USA

version: 3pm, 18 June 2000

ABSTRACT

This paper proposes a simple, empirically derived, unifying structure for the inner regions of quasars. This structure is constructed to explain the broad absorption line (BAL) regions, the narrow ‘associated’ ultraviolet and X-ray ‘ionized’ absorbers (NALs); and is also found to explain the broad emission line regions (BELR), and several scattering features, including a substantial fraction of the broad X-ray Iron-K emission line, and the bi-conical extended narrow emission line region (ENLR) structures seen on large kiloparsec scales in Seyfert images.

The model proposes that a funnel-shaped thin shell outflow creates all of these features. The wind arises vertically from a narrow range of radii on a disk at BELR velocities. Radiation force then accelerates the flow radially, so that it bends outward to a cone angle of $\sim 60^\circ$, and has an divergence angle of $\sim 6^\circ$, to give a covering factor of $\sim 10\%$. When the central continuum is viewed from the

side, through this wind, narrow high ionization ‘associated’ ultraviolet absorption lines and the X-ray ‘ionized absorbers’ are seen, as in many low luminosity active galactic nuclei. When viewed end-on the full range of velocities is seen in absorption with a large total column density, giving rise to the broad absorption lines systems seen in a minority of quasars, the BALQSOs.

The wind is both warm ($\sim 10^6$ K) and highly ionized. This warm highly ionized medium (WHIM) has a density of $\sim 10^9$ cm $^{-3}$, putting it in pressure equilibrium with the BELR clouds; the BELR is then a cool phase embedded in the overall outflow, avoiding cloud destruction through shear. The wind has the correct ionization parameter and filling factor for this. The high and low ionization zones of the BELR correspond to the cylindrical and conical regions of the wind, since the former is exposed to the full continuum, while the latter receives only the continuum filtered by the former.

The warm wind is significantly Thomson thick along the radial flow direction, producing the polarized optical continuum found in BALs, but is only partially ionized, creating a broad fluorescent 6.4 keV Fe-K emission line, and >10 keV

Compton hump. The conical shell outflow can produce a bi-conical matter bounded NELR.

Luminosity dependent changes in the structure, reducing the cylindrical part of the flow, or increasing the mean angle to the disk axis and decreasing the wind opening angle, may explain the UV and X-ray Baldwin effects and the greater prevalence of obscuration in low luminosity AGN.

1. Introduction

This paper proposes a simple unifying structure for the inner regions of quasars. It is almost universally acknowledged that a massive black hole lies at the core of all quasars, and it is widely believed that this black hole is surrounded by an accretion disk that emits the powerful continuum radiation characteristic of quasars. Yet the slightly larger region around the continuum source, which produces most of the prominent and much studied emission and absorption features in quasar spectra, is not well understood. It is this region that we address.

Any model of quasars and active galactic nuclei (AGNs) needs to explain self-consistently a wide range of emission and absorption line phenomena. At a minimum the pieces of this jigsaw include: the $\sim 5000 \text{ km s}^{-1}$ broad emission lines present in all AGN; the $\sim 0.1c$ ($\sim 30,000 \text{ km s}^{-1}$) broad absorption lines seen in some 10% of quasars; and the highly ionized $\sim 1000 \text{ km s}^{-1}$ outflows seen in narrow absorption lines in the ultraviolet and X-ray spectra of about half of Seyfert galaxies. This is a challenging array of observations, and they lead to constraints which are hard to satisfy. Each phenomenon has been the object of many studies that have defined its properties in detail over the last two or three decades. Still missing though is a structural and dynamic context that fits these apparently disjoint elements together (Peterson 1997; Krolik 1999). The most obvious geometries are a turbulent, spherical distribution of clouds and a rotating disk with an equatorial wind. While both structures have their successes, they also have problems. One difficulty in particular stands out: how can they explain the simultaneous presence of outflowing material at 1000 km s^{-1} and at $30,000 \text{ km s}^{-1}$ implied by the absorption lines?

Beginning from this puzzle we propose the following, phenomenologically based, geometric and kinematic structure: An accelerating outflow with a funnel-shaped thin shell geometry is responsible for all of these features. This is the simplest geometry that can explain both the broad and narrow absorption line observations. We find that having set up this structure it also explains a wide variety of other emission line and scattering phenomena. With minor extensions, this structure could also explain a number

of luminosity related effects.

The scope of this paper is to outline how this structural model can link these diverse phenomena empirically. In individual areas, preceding studies have often argued for the same or related conditions. Fitting all of these areas together has not been achieved before, and it is the structure proposed here that makes this possible. Many of the details and theoretical consequences are not investigated here, but are explored semi-quantitatively in the following sections to see if obvious conflicts with observation arise. At the end of the paper some theoretical work is referred to that promises to give the model a good physical basis.

2. Overview

In outline¹, a flow of warm gas first rises vertically from a small range of radii on an accretion disk rotating, tornado-like, with the initial Keplerian disk velocity, comparable with BEL velocities. The flow then angles outward, and accelerates to BAL velocities, until it makes an angle of $\sim 60^\circ$ to the quasar axis, with a divergence angle of $\sim 6^\circ \sim 12^\circ$ (figure 1). Viewed along the flow a BAL is seen. Dust in low luminosity objects prevents the BALs being seen in Seyfert 1 galaxies. (They appear as Seyfert 2s.)

Viewed across the flow NALs and X-ray warm absorbers are observed. Viewed from above no absorbers are apparent. The angles are set in order to produce the correct ratios of Narrow Absorption Line (NAL), Broad Absorption Line (BAL) and non-absorbed quasars. The medium is warm ($\sim 10^6$ K), has a high density ($n_e \sim 10^9 \text{ cm}^{-3}$), and is highly ionized, as required by X-ray observations. We call this the Warm Highly Ionized Medium (WHIM).

These properties make the WHIM the confining medium for the clouds of the broad emission line region (BELR), for which it has the correct pressure, ionization parameter, radius and filling factor. If the wind origin radii span a factor 2, with decreasing density at larger radii then the two zones of the BELR have a natural origin: the high ionization BELs originate primarily in the inner region where the clouds are exposed to the full ionizing continuum, while the low ionization BELs originate in the outer region where they are exposed only to the continuum filtered through the WHIM. An outflowing wind with embedded cooler clouds suffers none of the shear stress problems of fast moving clouds in a stationary atmosphere that have seemed to make pressure confined BELR clouds implausible, and the thin shell geometry avoids the Compton depth problem previously

¹For brevity all references are deferred to the following detailed discussion.

encountered in such models. The WHIM also produces the high ionization ‘coronal’ optical emission lines.

Along the conical outflow direction the WHIM has significant optical depth to electron scattering ($\tau \sim 1$), as required by spectropolarimetric observations of BALs and suggested by X-ray spectra. This allows the WHIM to be the source of some, and perhaps all, of the five scattering phenomena in AGN. Scattering off the far side of the flow explains (1) the $\sim 10\%$ polarized continuum seen in BAL troughs, and the 0.5% polarization of non-BAL quasars, and (2) the strong continuum polarization in the UV. In addition (3) the ‘mirror’ seen in the 20% of Seyfert 2 galaxies with polarized broad emission lines can have the same origin if, in low luminosity AGN, the flow is dusty. X-ray reflection features, (4) the ‘Compton hump’ above 10 keV and (5) the fluorescent Fe-K line at 6.4 keV will arise from continuum reprocessing in the warm conical shell wind, and will provide, at a minimum, a significant fraction of the observed features.

The model is summarized in figure 1. The top left quadrant of figure 1 (‘geometry’) shows the required angles. The top right quadrant of figure 1 (‘taxonomy’) shows which lines of sight give rise to which type of absorber, while the lower right quadrant (‘kinematics’) shows typical velocities. The lower left quadrant (‘physics’) shows the relevant column densities and optical depths.

This geometry arises naturally if a disk instability creates a wind. For example, radiation pressure dominates a disk inside a critical radius. At smaller radii something (e.g. a hot corona) must suppress the wind, leaving only a narrow boundary region on the disk from which the wind can escape. Centrifugal action and radiation pressure then bends and accelerates the flow. At large radii this geometry may produce the bi-conical narrow emission line structures.

High luminosity quasars differ from the lower luminosity AGN in several features: the lower CIV EW (Baldwin effect), the rarity of NALs, and the weakness of X-ray scattering features in high luminosity quasars. Small changes in the outflow shape (specifically in the outflow opening angle, divergence angle and the height of the cylindrical region), may explain these. Such shape changes could result from increased radiation or cosmic ray pressure at high luminosities.

3. Presentation of the Quasar Structure

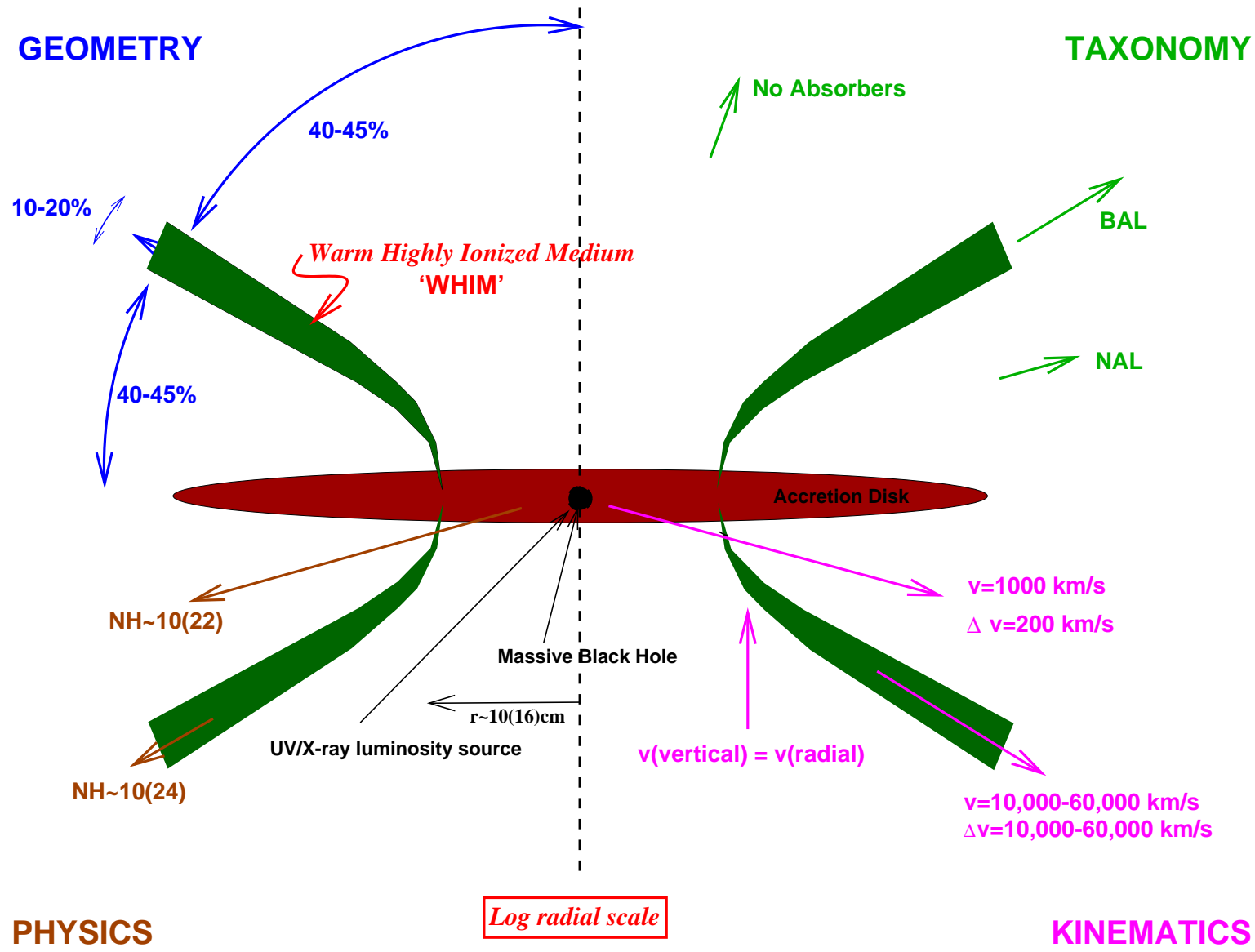


Fig. 1.— The proposed structure. The four symmetric quadrants illustrate (clockwise from top left): the opening angles of the structure; the spectroscopic appearance to a distant observer at various angles; the outflow velocities along different lines of sight; some representative radii (appropriate for the Seyfert 1 galaxy NGC 5548) and some typical column densities.

3.1. A Conical NAL Geometry

The intensely studied active galactic nucleus (AGN) NGC 5548 has had a NAL (of column density of $4 \times 10^{21} \text{ cm}^{-2}$) with a outflow velocity of 1200 km s^{-1} , for over 20 years without significantly altering its high ionization state (Shull and Sachs 1993; Mathur, Elvis and Wilkes 1999). Yet a radial flow would have at least doubled its distance from the ionizing continuum source over this time (figure 2a; Mathur, Elvis, and Wilkes 1995), which would increase the column density in the trace CIV ion by a factor of ~ 100 , contrary to observations. Continuous flow along the line of sight is ruled out, since the absorber is constrained to be thin in that direction [thickness $< 10^{15} \text{ cm}$, c.f. distance from continuum $= 2 \times 10^{15} - 2 \times 10^{18} \text{ cm}$, if the UV NAL and the high ionization (dominated by OVII, OVIII) X-ray absorption both arise in the same material (Mathur, Elvis, and Wilkes 1995)²]. Instead a steady state flow *across* our line of sight, with only a component of the velocity in our direction, provides a natural explanation for this constancy of ionization (figure 2b; Mathur, Elvis and Wilkes 1995, 1999).

We now note that, given the above ‘continuous flow’ requirement, the simplest geometry for the NAL in NGC 5548 is a thin bi-conical shell (figure 2c) with a radial outflow velocity that will be larger, possibly much larger, than shown by the NAL. The thinness of the shell implies that the flow arises at a limited range of radii on a disk. The opening angle of the conical shell is given by the ratio of NALs to absorption free AGN (1:1) (Reynolds 1997; Crenshaw et al. 1999). This ratio implies that the flow makes an angle of 60° to the disk axis, dividing the absorbed and unabsorbed solid angles equally (figure 2c)

3.2. Broad and Narrow Absorption Lines: two views of the same outflow

A conical outflow has three distinct viewing directions (figure 3.1c): above the cone, across the cone, and down the length of the cone. This third view will produce higher velocity absorption in a small fraction of quasars. The flow, if accelerated by radiation pressure must have a divergence angle, since the illumination is not parallel. For an angle of 60° to the pole, the flow will have a height comparable to its radius. The angle subtended to the accelerating continuum will be given by the thickness of the flow, which is ~ 0.1 radii,

² Statistically the UV absorption features and the X-ray warm absorbers are closely related (Crenshaw et al. 1999), and can even be used to predict one another’s presence (Mathur, Wilkes & Elvis 1998). The first *Chandra* absorption line results (Kaastra et al. 2000, Kaspi et al. 2000) show that the high ionization X-ray absorption lines also have outflow velocities matched to those of the UV absorbers. There remain difficulties in fitting the observed UV and X-ray line strengths with a one component model in some cases.

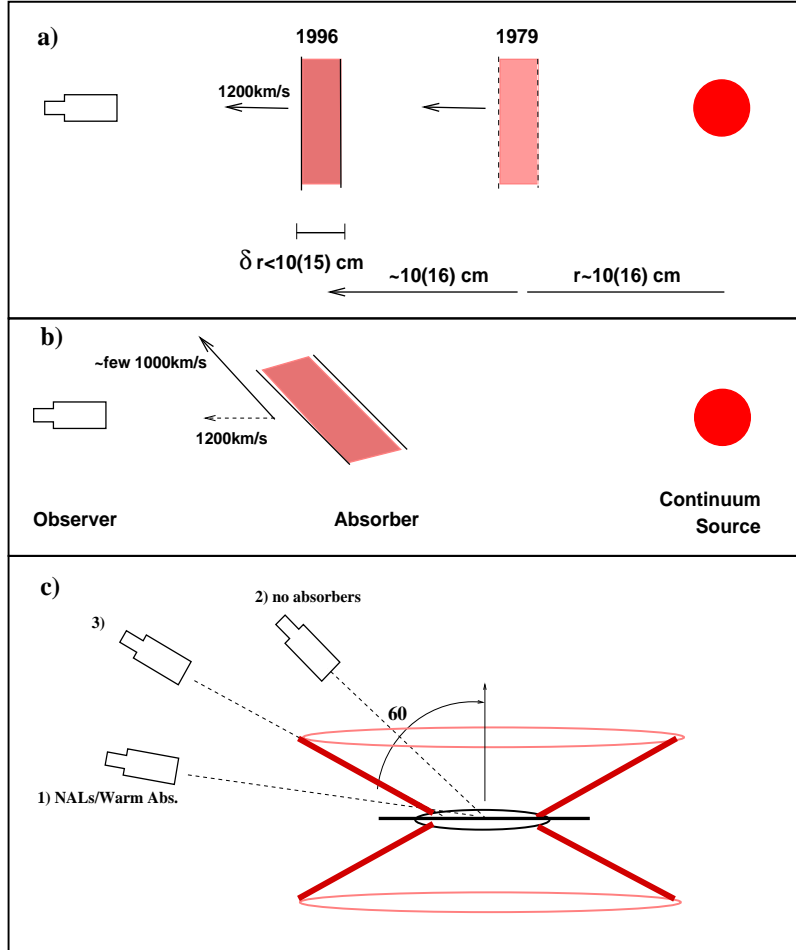


Fig. 2.— Geometry of the NAL/X-ray warm absorber: (a) Apparent outflow rate would double the continuum-absorber separation in 20 years, incompatible with observations. (b) A steady state flow crossing our line-of-sight reconciles the observations. (c) The simplest nuclear structure compatible with (b) is a bi-cone.

i.e. 6° , which implies a covering factor of ~ 0.1 . There is a population of quasars that shows these characteristics, the Broad Absorption Line quasars (BAL quasars).

All radio-quiet quasars seem to contain high velocity outflows ($v \sim 0.1 - 0.2c$, 10-20 times larger than NALs) as shown by studies of broad absorption lines (BALs) in quasars (Weymann et al 1991; Hamann, Korista, and Morris 1993). Any model of quasar structure must then include BAL outflows. BALs are observed directly in 10-20% of radio-quiet AGN and so cover a similar fraction of the solid angle around the continuum source (Weymann et al 1991; Hamann, Korista, and Morris 1993). The geometry of BAL flows is not known, but may well have conical shell geometries (Murray et al 1995; Ogle 1998).

We propose that NALs and BALs are two views of the same flows. In NALs we look across the flow direction, while in BALs we look down the length of the flow. BALs had been thought to have inadequate column densities ($\sim 10^{20}-10^{21}\text{cm}^{-2}$), similar to NALs, and relatively low ionization (Turnshek 1988). Now however X-ray results on broad absorption line quasars (BALQSOs) (Mathur, Elvis, and Singh 1996; Gallagher et al 1999, Mathur et al. 2000) strongly suggest absorbing column densities $\gtrsim \text{few} \times 10^{23} \text{ cm}^{-2}$, 2-3 orders of magnitude larger than expected from optical data alone. The relatively weak optical absorption then requires the BALs to have high ionization parameters, comparable with those of NALs (Hamman 1998). The detection of NeVIII, OVI and SiXII in some BALs (Telfer et al 1998) supports high BAL ionization parameters.

Variability studies give some support for the existence of large structures in quasars on this size scale: microlensing events in the double quasar Q0957+561 contain a low amplitude signal with delay times of 52–224 days (Schild 1996), implying luminous, possibly reflective, structure with a 10% covering factor on a size scale appropriate for being the BAL outflow (see §5); a continuum lag of 100 days is seen in NGC 3516 (Maoz, Edelson & Netzer 1999) also implying a reflecting structure on this scale.

A covering factor of 10% for BALs implies a divergence angle of 6° (figure 1, top left quadrant, ‘geometry’); 20% implies a wider angle of 12.2° . Continuity implies a decreasing density in the wind with radius which will maintain a constant ionization parameter, apart from the attenuation of the ionizing radiation by absorption and scattering.

A simple bi-cone though, is not compatible with the data. The velocity of the NALs, $v(\text{NAL}) \sim 1000 \text{ km s}^{-1}$ is only $\sim 1/20$ that of a BAL, implying that the typical angle through the flow at which associated absorbers are found is 87° , inconsistent with the angles derived above. The simplest geometry that removes this problem is to have the flow begin as a locally vertical flow, which is appealing on the grounds of symmetry. Most NALs then arise in a quasi-cylindrical region, and would be viewed almost directly across the flow

(figure 3.2). The cylindrical flow is viewed in NALs between 90° and 57° (figure 3.2) for a mean angle of 80° , so the vertical outflow velocity in this region is typically some 6 times greater than the observed NAL blueshift, i.e. comparable to the BELR velocities (FWHM). A cylindrical flow will inevitably curve outward at some point as vertically displaced gas elements will have excess kinetic energy for their increased radial distance from the central mass (deKool 1997). The whole flow then has a funnel-shape.

This shape has a natural physical interpretation. Radiation or cosmic ray pressure can cause the flow to bend radially outward and accelerate it to the large BAL velocities (deKool 1997). In this picture the onset velocities of BALs relative to the emission line peaks, occur at the point where the flow turns outward to become part of the BAL line-of-sight. This will happen when the radial velocity becomes comparable with the vertical velocity (figure 3.2). The range of vertical velocities will be similar to the BAL ‘detachment velocities’, $\sim 0\text{--}5000 \text{ km s}^{-1}$ (Turnshek 1988; Weymann et al 1991). N. Murray (2000, private communication) suggests that Low ionization BALs, which have narrower widths than high ionization BALs, might arise from a shielded low ionization region just outside the high column density X-ray ‘warm absorber’ producing part of the outflow, extending for about a factor 2 in radius. This arrangement of matter proves to be valuable in understanding BELR structure too (see 4.1).

4. Implications of the Structure

Given the structure just presented, other parts of the AGN puzzle fit quite naturally. Several of the solutions given below have been proposed individually before, and references are given, but they have not before all been fitted together in a single scheme, as here. The structure presented here allows the solution.

Figure 4 shows a 3-dimensional rendering of the structure. The multi-colored disk represents the accretion disk. The top figure shows the side view, viewing the continuum source through the cylindrical part of the flow, where absorption produces the NAL; the middle figure shows the view directly down the conical flow, where the accelerating flow produces a BAL spectrum; the lower figure shows the view over the top of the flow, where there is a clear line of sight to the continuum source. Embedded in the flow are small condensations which are the BEL clouds. We discuss these next.

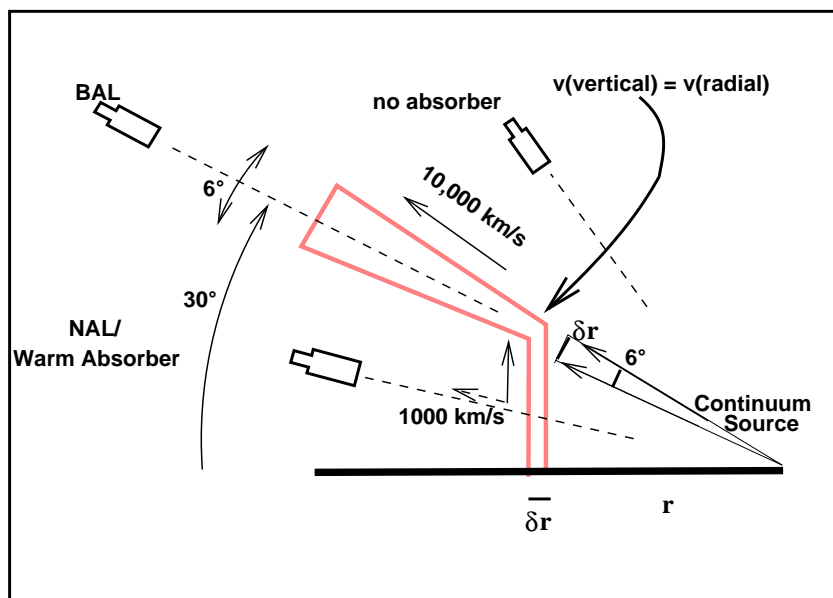


Fig. 3.— A ‘funnel’ is the simplest geometry that allows NALs and BALs to arise in the same outflow.

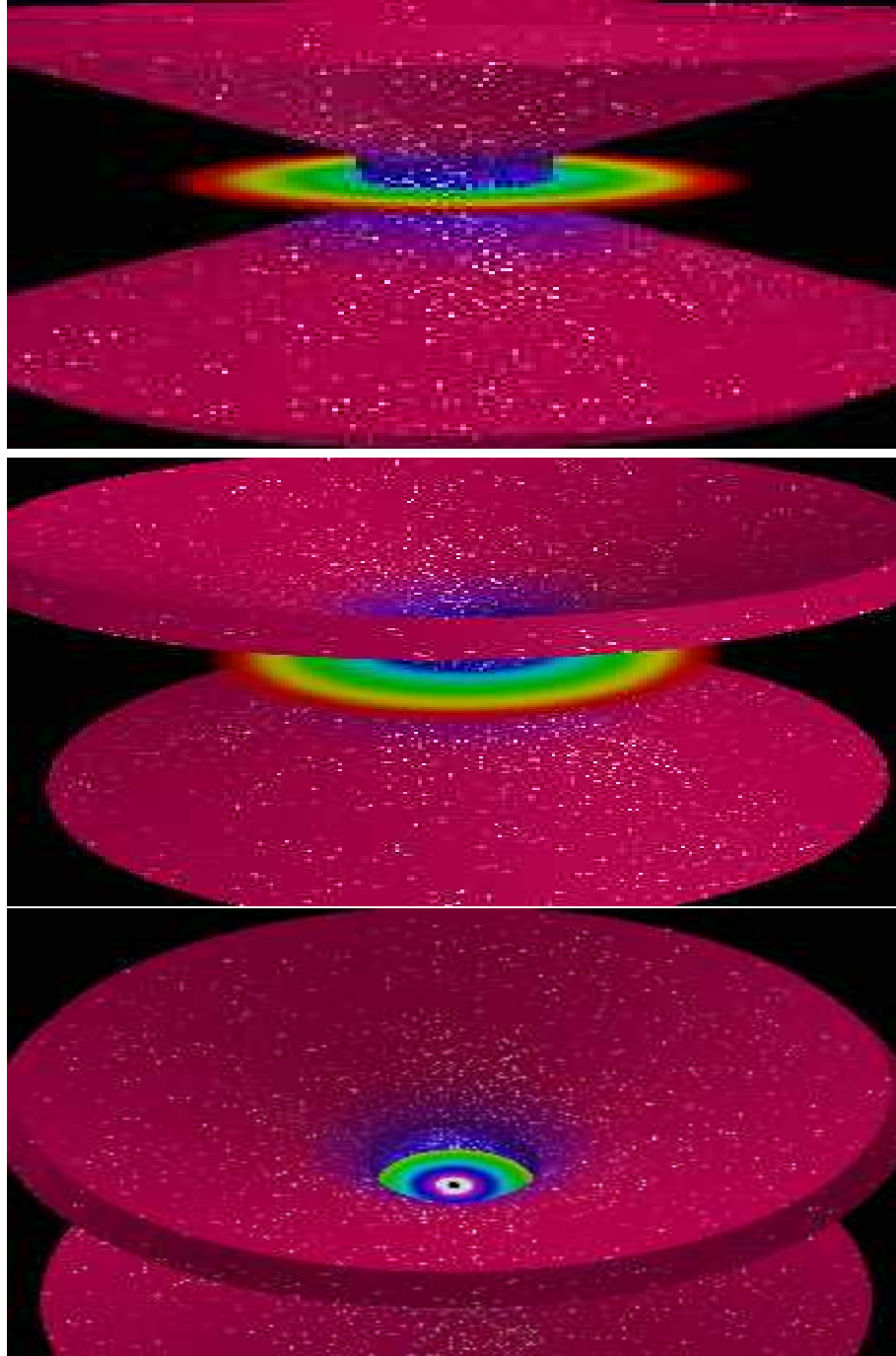


Fig. 4.— 3-dimensional views of the proposed structure: *top* from the side, through the NAL producing outflow; *middle* down the length of the accelerating, BAL-producing outflow toward the continuum source (note the visibility of a large area of the far side of the flow); *bottom* over the top with an unobscured view of the continuum source. The multi-colored disk represents the accretion disk. The small white dots represent BELR clouds embedded in the flow. (The sharp edges are an artifact of the 3-D rendering program.)

4.1. WHIM and BELR: two phases of the same Medium

The broad absorption line and broad emission line regions are closely related. Lee & Turnshek (1995) see a correlation of their line widths. Also the size of the high ionization BELR (in CIV) in NGC 5548 is 10 light-days (Peterson 1997), $\sim 10^{16}$ cm, consistent with the distance of the WHIM from the ionizing continuum (§3.1) (Mathur, Elvis, and Wilkes 1995).

Conditions in the WHIM and BELR are also suggestively related: A strong case can be made that the WHIM is sufficiently warm and dense that it can pressure confine the BELR clouds, as proposed here. Pressure confined BELR models have a long history (Matthews 1974) but are not currently favored (Peterson 1997). Nevertheless the case for high ionization material in the vicinity of the BELR has been well argued by Shields, Ferland & Peterson (1995) and by Hamann et al (1995a,b) who detected broad NeVIII emission lines. That the NAL medium confines the BELR clouds has been suggested before (Turner et al 1993; Kaastra, Roos and Mewe 1995; Marshall et al 1997). Additional evidence for high pressure, combined with the geometry proposed here, now make the case stronger.

The evidence for the WHIM having a high pressure comes from X-ray absorption and emission features. X-ray absorption edges in some AGN fail to respond immediately and linearly to changes in the ionizing continuum as expected in equilibrium photoionization models (Fabian et al 1994; McHardy et al 1995). Both non-equilibrium models and warm absorbers at $\sim 10^6$ K (where collisional ionization competes with photoionization) can reproduce these changes, and both require quite high densities, $10^6 < n_e < 10^8$ (Nicastro et al 1999). Higher densities are needed in AGN where no delays are seen, (e.g. NGC 5548; Nicastro et al 2000).

Strong high ionization OVII emission lines are seen in soft X-rays in the Seyfert 1 galaxies NGC 5548 and NGC 3783 (George et al. 1995, Nicastro et al. 2000, Kaspi et al., 2000, Kaastra et al., 2000). However, a spherical geometry would produce EUV and X-ray emission lines that were much too strong. Kaastra et al. (1995) find a filling factor for the WHIM of $\sim 0.5\%$, in reasonable agreement with the 1% of a conical shell with a 6° divergence angle. To explain these lines requires a thermal ionization component at $T \sim 10^6$ K and $n_e \sim 10^9$ cm $^{-3}$ (George, Turner, and Netzer 1995; Nicastro et al 1999). This thermal gas has the correct ionization state and column density to produce the X-ray absorbers and the UV NALs (Kaastra, Roos, and Mewe 1995)³. The pressure in the WHIM

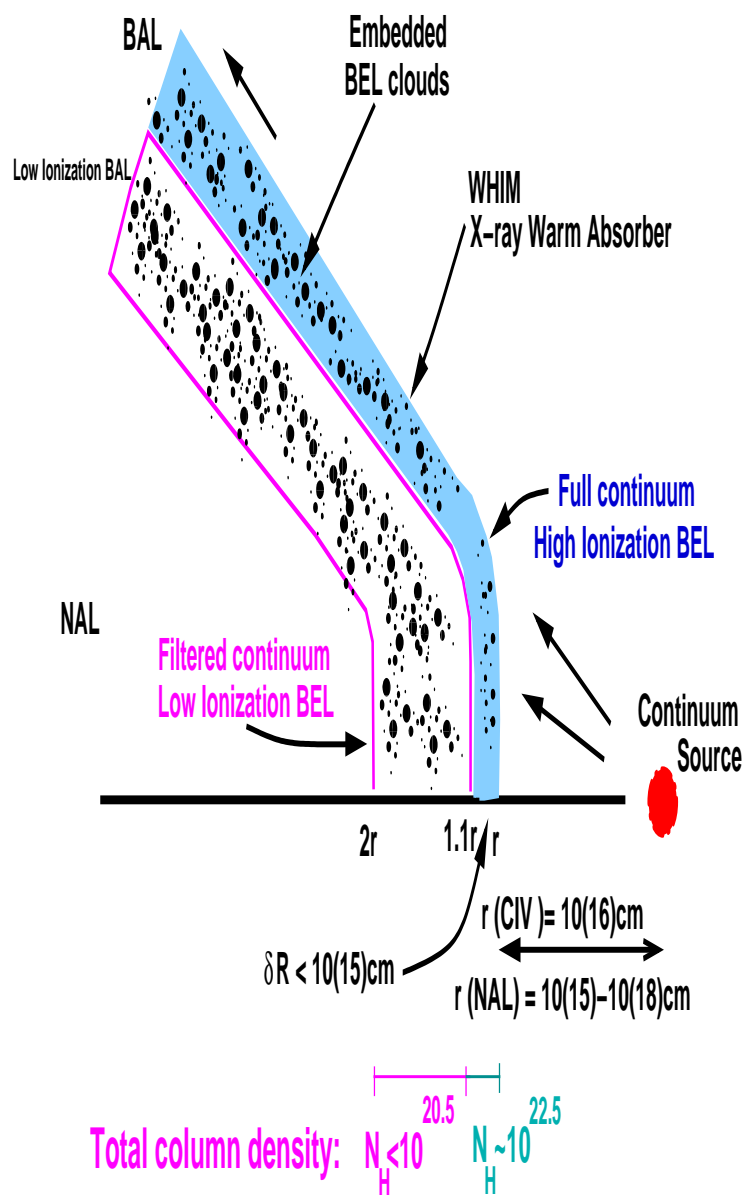
³ The EUV NeVII/NeVIII blend, SiVII emission lines reported in NGC 5548 by Kaastra, Roos & Mewe (1995) have been disputed by Marshall et al. (1997). However, the conditions they derive are sufficiently

of the ionized absorbers in the NGC 5548 is $P_{WHIM} = 10^{15} \text{ cm}^{-3} \text{ K}$, which is comparable to the pressure in the BELR (Osterbrock 1989; Ferland et al 1992), $P_{BELR,CIV} = 10^{15} \text{ cm}^{-3} \text{ K}$. The factor ~ 100 higher density in the BELR requires that the ionization parameters of the WHIM, U_{WHIM} be a factor ~ 100 , higher than that of the BELR, U_{BELR} . This is close to the observed factor of 50 ($U_{BELR,CIV} = 0.04$ Peterson 1993; $U_{WHIM} = 2$; Mathur, Elvis and Wilkes 1995). This may well be generally true, since NALs (Crenshaw et al. 1999) have quite uniform U as do BELRs (Osterbrock 1989). Kaastra et al. (1995) find (independent of their EUVE data) that for the observed NGC 5548 continuum a 2-phase medium forms at the distance of the BELR, with $T = 5 \times 10^4 \text{ K}$ and $T = \text{few} \times 10^5 \text{ K}$, a slightly narrower range than above, but in good qualitative agreement, given the poorly known continuum from $100\text{\AA} - 912\text{\AA}$.

If the outflow spans a factor 2 in radius then the two BELR zones deduced from observation (Collin-Souffrin et al. 1988, Goad et al. 1999) are created naturally (N. Murray 2000, private communication). These zones are: the ‘high’ ionization zone (e.g. CIV) and the ‘low’ ionization zone (e.g. MgII) (figure 3, which has large optical depth and is mostly heated and ionized by hard X-rays (Collin-Souffrin et al 1988). The WHIM filters the ionizing continuum, preventing soft X-ray flux (Ferland et al 1990) reaching the outer radii. This is appealing since the low ionization lines have somewhat narrower widths (FWHM) than high ionization lines, which would arise from the $\sqrt{2}$ lower Keplerian disk velocities at double the radius, and is consistent with the line width vs. inverse square-root of the lag time relation found for several Seyfert galaxies (Peterson & Wandel 1999, 2000). A zone of about the correct width was noted by Nicastro (2000) in his model which relates BEL width to Keplerian disk velocity which uses the disk instability model of Witt, Czerny, & Źycki (1997) (see §6.4).

How can a factor ~ 2 in radius be reconciled with the thin shell required by the X-ray observations? The thin shell applies to the high ionization ‘warm absorber’ zone. A lower density spanning a wider range of radii is allowed so long as the total column density through the low ionization region is small enough not to have significant optical depth in soft X-rays, notably in oxygen, i.e. $N_H \leq 10^{20.5} \text{ cm}^{-2}$. Since the warm absorbers have $N_H \sim 10^{22} \text{ cm}^{-2}$ a strong radial density gradient in the outflow is required. In the model of Witt, Czerny, & Źycki (1997) a gradient will be present, but may not be sufficiently steep (B. Czerny, 2000, private communication). Evidence for cold absorption associated with warm absorbers has been seen in several X-ray spectra (Komossa 1999), and has been modelled with dust absorption, though low N_H cold gas may also be allowed. If this is

close to those required from the X-ray OVII and variability data, that their other conclusions apply. We predict then that the lines they report will be found with observations of slightly greater sensitivity.



confirmed then the steep density gradient requirement may be lessened.

Some low ionization line emission could arise along the conical flow, several light-months away from the continuum source (for NGC 5548), which also will be shielded from the full continuum by the WHIM. MgII in NGC 3516 has a reverberation time comparable with these sizes (Goad & Koraktar 1997). In this case though the WHIM is being accelerated and so the lines should appear broader. A low contrast ‘Very Broad Line Region’ (VBLR) is present as shown by variability (Ferland, Korista, and Peterson 1990) and polarimetry in some AGN (Goodrich and Miller 1994; Young et al 1999) with about double the width of the normal (variable, unpolarized) BELR. These lines may arise in the conical flow region.

Models in which the BELR clouds are confined in pressure equilibrium in a 2-phase medium (Krolik, McKee and Tarter 1981) have fallen out of favor due to lifetime problems (Matthews 1986) and high Compton depth. In the thin shell steady state outflow picture presented here the geometry gives a medium which has a low Compton depth except along the flow. Moreover, the individual clouds do not need long lifetimes, since they leave the BEL emitting, vertical, part of the flow on an outflow timescale, comparable to the dynamic timescale. Moreover they are not pulled apart by strong drag forces, since they co-move with the confining medium. Only a small energy input, $\sim 10^{-4}$ relative to the bulk kinetic energy of the outflow, is needed to heat the NAL gas to 10^6 K.

Radiation driven flows commonly suffer instabilities and shocks (e.g. Williams 2000) which may well heat the WHIM (e.g. Feldmeier et al 1997), and may also produce the fine structure in the absorption line velocity profiles seen in NALs (Mathur, Elvis and Wilkes 1999; Crenshaw and Kraemer 1999) and BALs (Turnshek 1988). In BALs the constancy of this velocity structure (Weymann 1997) suggests standing shocks, although in NALs fine structure variability has been seen arguing for some transverse motions (Crenshaw et al. 1999). Shock heating along the flow may also prevent the rapid adiabatic cooling of the WHIM. If the WHIM were in free expansion at the hot phase sound speed ($v(10^6\text{K}) \sim 200 \text{ km s}^{-1}$) and was moving away from the continuum source at $v(\text{outflow}) \sim 20,000 \text{ km s}^{-1}$ in order to make BALs, then an opening solid angle of only 1% will result. The flow must then be forced into supersonic lateral expansion by some extra pressure, perhaps magnetic, to cover the necessary 10%–20%.

If we provisionally accept the identification of the BELR as condensations in the larger WHIM outflow, is this consistent with the known properties of the BELs? Emission lines give weaker constraints than absorption lines because the information they carry has been integrated over a volume distribution of material, rather than a line, convolving together ranges of density and ionization state to produce the emission line. The prediction of BEL profiles is thus subject to the uncertainties of many parameter models. Nevertheless

a funnel-shaped distribution for the BELR seems to be consistent with the BEL profiles and widths. The distribution of BEL widths can be reproduced well by axisymmetric, but non-spherical, geometries (Rudge and Raine 1998), while the broad emission line profiles arise naturally in a wind (Cassidy and Raine 1993; Murray and Chiang 1995). The model predicts orientation effects in BEL profiles. Edge-on AGN, which will show NALs, will be dominated by the disk Keplerian velocities, while pole-on AGN, which will have no absorption features, will be dominated by the outflow velocities, both vertical and radial. Velocity resolved reverberation mapping of the ‘edge-on’ (because of the presence of NALs, figure 1, top right quadrant) AGN NGC 5548 (Korista et al 1995) shows that radial motion does not dominate for the CIV line. The cylindrical structure proposed here for the high ionization BEL will be rotating with the disk, so rotation will dominate in a NAL AGN, although a vertical velocity component will also be present. There is a tendency for high ionization lines to be blueshifted relative to low ionization lines (Peterson 1997; Wilkes 1984), which has no obvious interpretation in this model.

The observation that the NALs absorb the BELs (Mathur, Elvis, and Wilkes 1999; 1995) presents a difficulty, since it suggests that the NAL is exterior to the BEL, rather than being co-mingled. Several authors have noted though that this problem is avoided if the BEL clouds primarily emit back toward the continuum, and so are seen originating on the far side of the flow (Hamann, Korista, and Morris 1993; Shields 1994; Shields, Ferland, and Peterson 1995) and are seen through the near side.

5. A Single Compton Thick Scatterer

Active Galactic Nuclei give ample evidence for scattering and fluorescing media: (1) BAL quasars have 5%-10% polarized flux filling in the BAL troughs (Cohen et al 1995; Goodrich and Miller 1995; Ogle 1998), requiring an ionized medium with significant electron scattering optical depth ($\tau > 1$, $N_H > 1.5 \times 10^{24}$); (2) some type 2 Seyferts have highly polarized broad lines (Antonucci and Miller 1985; Miller and Goodrich 1990) due to electron scattering ($\tau > 0.1$) off a warm ($T \sim 3 \times 10^5$ K) medium (Miller, Goodrich, and Mathews 1991); (3) X-ray spectra of Seyfert 1 galaxies often show an excess ‘hump’ of emission above 10 keV ascribed to Compton scattering ($\tau \gtrsim 1$) (Piro, Yamauchi, and Matsuoka 1990; Pounds et al 1990; Lightman and White 1988); (4) a broad fluorescent Fe-K line is seen in many Seyfert 1 X-ray spectra peaking around 6.4 keV (i.e. no more ionized than FeXVII), but extending down in a long tail to $\sim 4\text{--}5$ keV (Tanaka et al 1995; Nandra et al 1997b) with implied Doppler velocities of up to $\sim 0.3 c$; (5) rapidly rising UV continuum polarization toward short wavelengths is seen in several quasars (Impey et al 1995; Koratkar et al 1995).

It seems unlikely that such an abundance of scattering phenomena should all be independent, although *a priori* they could be, and are usually modelled as such. The X-ray features are normally, and plausibly, thought to arise in the inner regions of an accretion disk, producing GR-distorted radiation (Bromley, Miller & Pariev 1998); the Seyfert 2 scatterer is believed to be an extended, 1–50 parsec scale, cloud (Miller, Goodrich, and Mathews 1991; Krolik and Kriss 1995); and the BAL scatterer is assumed to be part of the BAL outflow (Goodrich and Miller 1995). The UV continuum scatterer has been successfully modeled as a mildly relativistic outflowing wind from an accretion disk (Beloborodov and Poutanen 1999), a situation strongly reminiscent of the model proposed here. The WHIM outflow has many of the characteristics of all of these scatterers: high temperature and ionization, a significant Compton depth, substantial covering factor, and large velocities. The outflow must then contribute to these features. Can it explain them entirely?

5.1. BAL Scatterer

In a BAL quasar, where we observe down the flow, the conical shell outflow will produce an electron scattered continuum from the far side of the outflow (figures 4c, 5) which reaches a maximum 10% polarization for a cone angle of 60° from the disk axis (Ogle 1998), the same angle we find from other considerations (see §2). This component will appear at all energies, including X-rays, where it will reduce the apparent column density in existing X-ray spectra (Goodrich 1997b). Viewed from any non-face-on angle above the flow, this conical geometry will produce a slight net polarization that can account (Ogle 1998) for the weak (0.5% mean) optical polarization of non-BAL radio-quiet quasars (Berriman et al., 1990). Spectropolarimetry already suggests that the BAL scatterer is comparable in size to the BELR and may be cospatial (Goodrich and Miller 1995; Ogle 1997, 1998; Schmidt and Hines 1999).

5.2. Seyfert 2 mirror

The ‘mirror’ in Seyfert 2 galaxies with polarized BELs has comparable temperature, column density and outflow velocity to the NALs (Beloborodov and Poutanen 1999; R.Antonucci 1999, private communication). If, like BALs, the ‘polarized BEL’ Seyfert 2s are viewed end-on through the flow then, as in BALs, the polarized emission will be scattered off the far side of the flow.

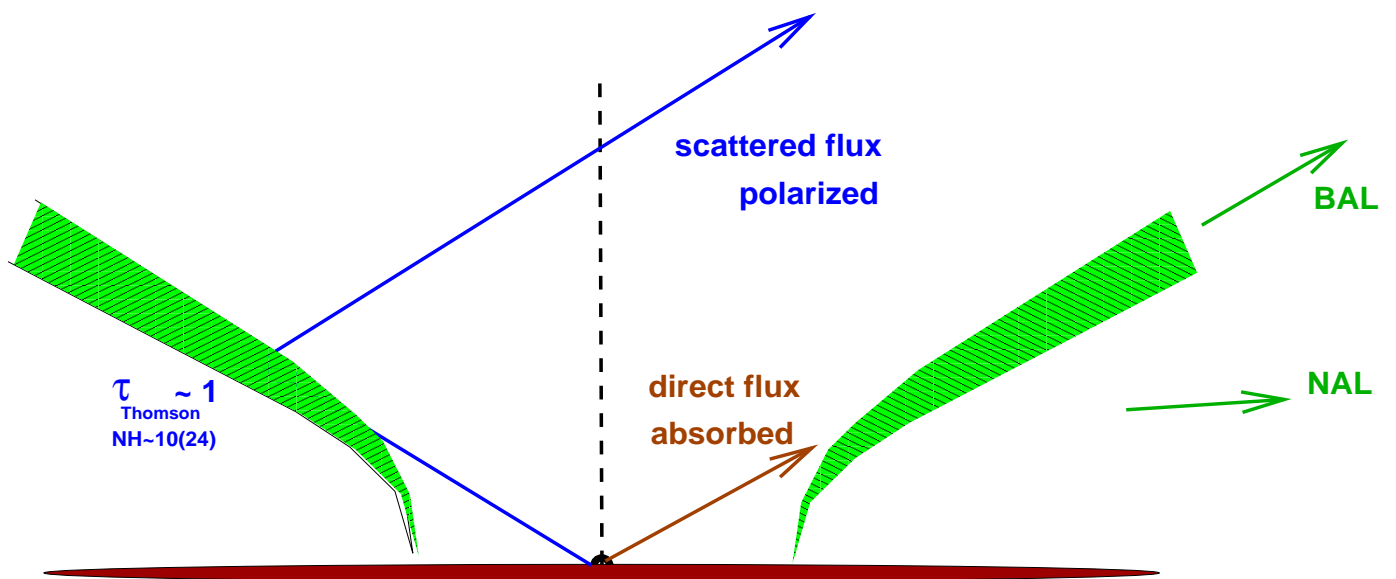


Fig. 6.— Geometry of Thomson scattering off the flow. (see also Ogle 1998.)

Dust may be more abundant in low luminosity Seyferts than in quasars (Edelson, Malkan and Rieke 1987), suggesting that Seyfert BALs are not detectable because reddening removes the UV spectrum where BALs are found, so making BALs rare in Seyferts, but relatively common in (radio-quiet) quasars (Turnshek 1988). [At least some of the long sought ‘quasar 2s’ (Almaini et al 1995; Halpern and Moran 1998) are then the BAL quasars.] About 20% of Seyfert 2s have polarized BELs (Kay 1994), however type 2 Seyferts are ~ 4 times as common as type 1s (Huchra and Burg 1992; Rush, Malkan, and Spinoglio 1993; Comastri et al 1995) so there are $\sim 80\%$ as many ‘polarized BEL’ Seyfert 2s as all Seyfert 1s, implying a covering factor close to 50% (see §6.2). The absence of large velocity shifts in the polarized BELs of Seyfert 2s is not surprising since the opposite side of the outflow is almost perpendicular to the line of sight. Large transverse outflow velocities will produce a second order Doppler shifts. This could explain the 400 km s^{-1} redshift of polarized $\text{H}\beta$ in NGC 1068 (Miller, Goodrich, and Mathews 1991) if the transverse velocity is $15,000 \text{ km s}^{-1}$. Spatially resolved Seyfert 2 mirrors (Capetti, Macchetto, and Lattanzi 1997; Capetti et al 1996) on a $\gtrsim 10$ parsec scale are probably too large to be a part of this structure, and have good alternative explanations (e.g. the 70 pc scale, warped molecular disk in NGC 1068, Schinnerer et al., 2000).

5.3. X-ray Scatterer

Disk models for the X-ray broad Fe-K line and Compton hump have difficulties in producing strong enough Fe-K emission lines. Several theoretical explanations have been proposed (stronger fluorescence from ionized plasma (Matt, Fabian, and Ross 1991; Źycki and Czerny 1994); enhanced abundances (Turnshek et al. 1996, but see Hamann, Korista and Morris 1993, Lee et al. 1999)⁴; anisotropic emission (George and Fabian 1991), but all have difficulties. The Seyfert galaxy IC4329A can have only a thin (half opening angle $< 10^\circ$) torus (Madejski et al., 2000). The inclusion of an additional Compton thick region, as given by the proposed outflow, may solve this problem. The conical outflow has a $0.2c$ velocity spread (defined by the BAL widths), which is almost as large as the reported broad Fe-K X-ray line widths, while also having the proper ionization state, with Fe-XVII dominating (Nicastro et al 1999). The 10% -20% covering factor of the BALs is 2-5 times lower than those of disk models and so would produce proportionately weaker Fe-K lines and Compton humps. [Although, as noted above (§5.2), a covering factor closer to 50% may be more appropriate for the low luminosity AGNs, in which broad Fe-K has been found.] 20%-40% of the observed Fe-K and Compton hump features could then arise in the outflow

⁴In fact enhancements of >4 times solar are excluded by the X-ray measurements.

structure.

Outflow models for the broad Fe-K lines have been considered previously: Fabian et al. (1995) noted that the strong observed red asymmetry of the broad Fe-K lines could be produced from the far side of the flow. With a transverse column density $N_H \sim 10^{22} \text{ cm}^{-2}$, $T \sim 10^6 \text{ K}$ and turbulent velocities $< 10^3 \text{ km s}^{-1}$ the WHIM is optically thick in the FeXXV resonance line and so to locally emitted FeXXV fluorescence. Redshifted FeXXV instead falls in the continuum where the WHIM is optically thin. In this condition red asymmetric lines may well be seen in NAL quasars, although detailed calculation is needed to produce reliable line profiles. However, Fabian et al. rejected outflow models both because of their *ad hoc* nature, and because of an apparent conflict with the smaller NAL velocities seen in the same objects. Our model removes both objections (§3.2): the outflow is already required to explain other quite different, absorption line, phenomena; and our geometry reconciles the low absorption line velocity across the flow, with the large emission line velocity width integrated along the flow.

While the size of the WHIM outflow permits variations of the broad Fe-K line over months, Fe-K line variability by a large factor on a timescale of days would limit the contribution from the extended conical shell outflow. Some broad Fe-K lines may show such variations (Iwasawa et al 1999; Wang et al 1999), while others do not (Georgantopoulos et al. 1999, Chiang et al. 2000), including the Seyfert galaxy NGC 7314 which shows apparent 1-day variability at low Fe-K velocities, but not at high velocities (Yaqoob et al 1996). IC4329A was studied simultaneously with ASCA and RXTE, so covering the Fe-K line and Compton hump with good S/N, making it a particularly good example (Done et al., 2000). In this observation the Fe-K line is clearly broad but, with a width of $\sim 23,000 \text{ km s}^{-1}$, it is distinctly narrower than a relativistic disk fit. The line also does not vary when the continuum changes by a factor 2. In a disk-torus scenario this behavior is puzzling. If a substantial fraction of the broad Fe-K line arises from the BAL outflow then the lack of response of the Fe-K line to continuum changes in these cases can be understood.

6. Discussion

6.1. Building BAL Column Densities

The expanding flow of figure 1 naturally creates a larger column density along the flow than across it. Integrating the column density with mass conservation gives a factor increase of $1/\theta$ radians, where θ is the flow divergence angle. (The $1/r^2$ decrease in density renders the contributions to column density from the outer parts of the flow negligible.)

For $\theta=6^\circ$ this gives a factor ~ 10 , i.e. $4 \times 10^{23} \text{ atoms cm}^{-2}$ for NGC 5548. This is somewhat less than a Thomson depth, $1.5 \times 10^{24} \text{ atoms cm}^{-2}$, implying $\tau_{es}=0.25$ and an scattering of 23% of the incident flux. This is somewhat low to create the observed scattering effects, and more detailed calculation is needed to test whether a larger column density is required.

A higher column density outflow could be created by adding mass to the WHIM. The BEL clouds offer a way of doing this. Once they enter the radial part of the flow the BEL clouds become shielded by a larger WHIM column density, so making the continuum they see weaker in soft X-rays. Nicastro (1995) has looked at the effect of steepening the ionizing ultraviolet to X-ray slope (α_{OX}) on the 2-phase medium, and finds that the instability disappears below some critical α_{OX} . If this applies in the conical part of the flow then the BEL clouds will disperse, increasing the total column density. In order to increase the column density by a factor 5-10 the mass in the BEL clouds has to be 5-10 times greater than in the WHIM. As yet there is no theory for the amount of matter that goes into each phase of a multi-phase medium such as the quasar outflow or the galaxy interstellar medium, so that a factor of this size is acceptable. BEL clouds need a minimum column density of 10^{22} cm^{-2} (Krolik 1999), but there is no upper limit and large values are sometimes invoked (Ferland et al., 1992). This allows large values of $M(\text{BEL clouds})/M(\text{WHIM})$, depending on the size and number of the clouds. Using the same simplifying assumptions as Peterson (1997), and a cylinder of thickness 1/10 of its radius for the vertical part of the flow, gives: $\frac{r(\text{BELcloud})}{r(\text{cylinder})} = 66N_{\text{cloud}}^{-\frac{1}{3}}$. So for $N_{\text{cloud}} = 10^6$, $\frac{r(\text{BELcloud})}{r(\text{cylinder})}=0.04$, and $r(\text{BELcloud}) = 4 \times 10^{14} \text{ cm}$, roughly 10 Schwarzschild radii (r_s) for a $10^8 M_\odot$ black hole, as deduced to be present in NGC 5548 from reverberation mapping (Ho 1998). For 10^9 clouds these dimensions become $\frac{r(\text{BELcloud})}{r(\text{cylinder})}=0.004$, $r(\text{BELcloud}) = 4 \times 10^{14} \text{ cm} \sim 1r_s$. Smooth BEL profiles favor $N_c > 10^7$ (Arav et al. 1998). These then are plausible numbers.

Alternatively there might be a reservoir of more highly ionized gas in the outflow. This is hinted at in the reports of an Fe-K absorption edge in some Seyferts (Costantini et al. 2000, Vignali et al., 2000). In this gas all elements up to iron are fully ionized. Such a medium would add to the Thomson depth and Fe-K fluorescence line strength without affecting the line absorption in soft X-rays or the UV.

6.2. Luminosity Dependences: the Baldwin Effect

High luminosity quasars differ from the lower luminosity Seyfert galaxies in several ways: (1) High luminosity quasars have weaker emission line equivalent widths, especially high ionization emission lines (Osmer and Shields 1999; Espey and Andreadis 1999), than low luminosity quasars (the ‘Baldwin Effect’; Baldwin 1977). (2) In X-rays the weakness of

Fe-K lines and Compton humps in quasars is consistent with the Baldwin effect (Iwasawa and Taniguchi 1993; Nandra et al 1997a). (3) NALs (in either UV or X-rays) are rare in quasars, but common in the lower luminosity Seyferts (Mathur, Elvis, and Wilkes 1999; Nicastro et al 1999).

We suggest that these three luminosity dependent effects are directly related to changes in the funnel geometry (figure 6.2). The angles derived so far (figure 6.2b) depend primarily on the statistics of NALs among Seyfert 1 galaxies, which are AGNs of relatively modest luminosity. If the quasi-vertical flow region is smaller at high luminosities (perhaps because radiative acceleration is stronger for high luminosity objects) then a smaller solid angle will be exposed to the unattenuated continuum source, weakening the BELR, particularly the high ionization lines. There will also then be a smaller solid angle from which the continuum can be viewed through the WHIM, so NALs will be rarer. If the cone opening angle is also larger at low luminosities then larger X-ray features will be produced, as noted above. A larger opening angle is suggested by the greater number of ‘polarized BEL’ Seyfert 2s compared with BALs (§5).

6.3. Biconical Structures and the Molecular Torus

For simplicity we have ignored the presence of accretion disk flaring and of the molecular torus which is commonly invoked (Antonucci and Miller 1985; Pier and Krolik 1992): (1) to explain the presence of polarized broad line emission in otherwise narrow lined (type 2) AGN (§5); (2) to collimate the ionizing radiation that leads to kpc-scale ionization cones of the extended narrow line region (ENLR, Tadhunter and Tsvetanov 1989); and (3) to create the observed 4:1 ratio of obscured (type 2) to unobscured (type 1) AGN (§5). If we allow the accretion disk or the torus to cover a large fraction of the sky as seen from the continuum source then the angles in figure 1 will be raised toward the axis substantially. However direct evidence for a nuclear torus is weak. The maser source in NGC 4258 shows clearly that a thin molecular disk is present in some AGN down to the 1 pc scale (Greenhill et al. 1999), but does not show that a thick 2π covering torus is present.

Overall the need for a torus is weaker in this model: (1) We have seen that the Seyfert 2s with polarized BEL could be viewed through a dusty BAL (§3.2) and that other, larger scale, asymmetric obscuring structures (e.g. the 70 pc-scale warped molecular disk resolved in NGC 1068, Schinnerer et al. 2000) can also produce polarized BEL spectra; (2) the conical shell outflow could itself produce the ENLR bi-cone structures, which would then be hollow matter bounded cones (as suggested by Crenshaw & Kraemer 2000 for NGC 5548), rather than filled, ionization bounded structures; (3) the other, more common,

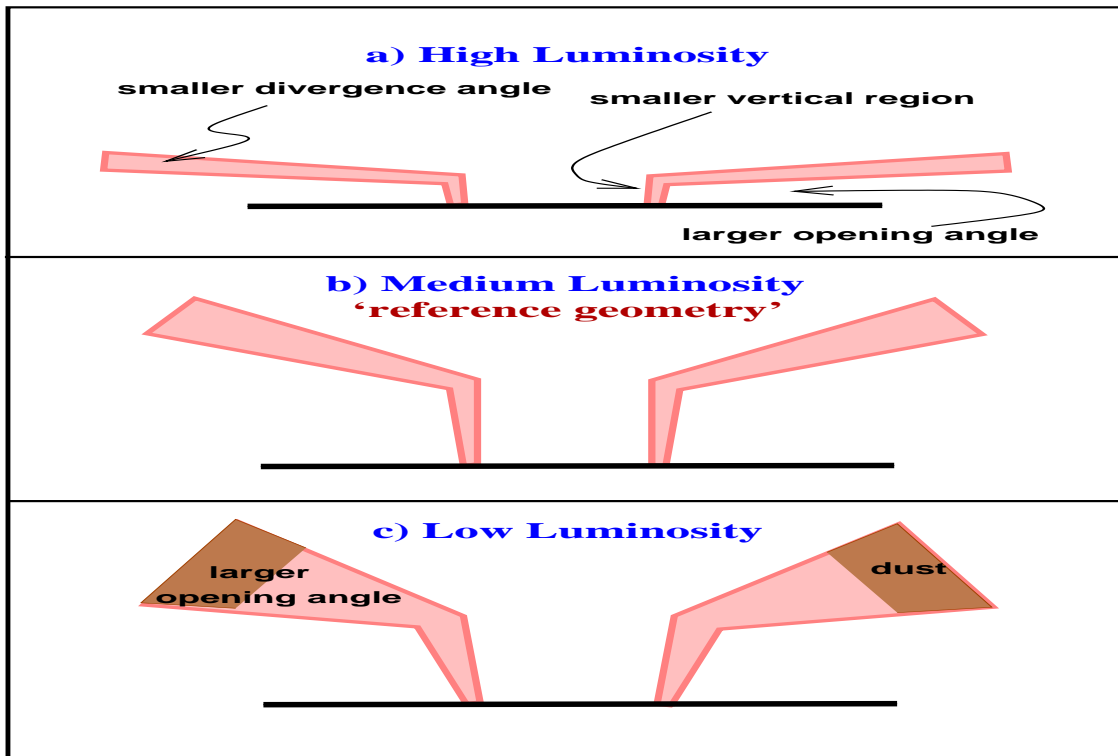


Fig. 7.— Luminosity dependent changes in the outflow structure that would account for observed luminosity correlations.

Seyfert 2s could be made in any of several ways: (a) the large narrow emission line region NELR endures \sim 1000 year after the central source is extinguished (Lawrence & Elvis 1982); (b) obscuration by large scale structures in the host galaxy disks (Lawrence and Elvis 1982; Maiolino and Rieke 1995; Simcoe et al 1998) or (c) in irregular non-nuclear obscuring clouds (Malkan, Gorgian & Tam 1998, REF 2000) can hide the small BELR but not the much larger NELR in many AGN.

The structure presented here is not directly inimical to the obscuring torus model, but a torus is less strongly required. The WHIM outflow could in fact be considered as a form of the obscuring torus.

6.4. Discriminating between Wind Models

Wind models for quasars have become widely discussed in recent years (see reviews by deKool 1997, Vestergaard 2000). In particular the detailed models proposed by Murray, Chiang and co-workers (Murray et al 1995; Murray and Chiang 1995, 1998), by Cassidy & Raine (1996) and, for binary systems, by Proga, Stone, and Drew (1998, 1999) have many features in common with the empirical picture developed here. This confluence is encouraging. Murray et al. have a wind emerging from all disk radii and accelerated into a wide cone by radiation pressure, which shows BAL when viewed edge-on. The key geometric difference is that the wind proposed here originates from a narrow range of radii and rises almost vertically before bending outward into a cone. This allows the NALs to be produced by viewing the flow edge-on. The main physical difference is that Murray et al. and Cassidy & Raine have a single phase medium. Murray et al. have different ionization states being produced from a wide range of footprint radii, producing a radially stratified BELR. The flow proposed here instead forms a 2-phase medium which originates in a narrow footprint and the high and low ionization zones are created from shadowing of the continuum by the WHIM. Ionized absorbers are hard to produce from a radially stratified BELR, unless the density gradient is large (§4.1), since we will always be looking through low ionization material too, which is X-ray opaque. However, the hydrodynamic models of Proga, Stone and Drew (1998, 1999), Proga, Stone & Kallman (2000) show, under some conditions, ‘streamer’ like high density structures that resemble the structure proposed here. Detailed calculation may then show the models are identical.

A related class of models, hydromagnetic wind models, use a magnetic field anchored in the disk to accelerate particles along field lines by centrifugal action (Emmering, Blandford & Shlosman 1992, Campbell 1999). Bottorf et al. (1997) begin with molecular material that is thrown up from the disk and becomes exposed to the ionizing continuum, so creating

broad emission lines as the clouds are accelerated along the field lines. In these models, as in the Murray et al. model, the range of radii from which material exits the disk is large.

6.5. Instabilities and Acceleration

Several instabilities are known that might create a wind from special radii of an accretion disk. The Lightman-Eardley radiation pressure instability zone in the accretion disk produces a wind originating within a critical instability radius, and the velocities at this radius are comparable to the BELs (Nicastro 2000). The stabilizing effects of a corona may restrict the range of radii in this model. External radiation of the disk can also create a wind from a restricted range of radii at about the correct radius (Begelman, McKee, and Shields 1983; Kurpiewski, Kurasczkiewicz and Czerny 1997).

Nicastro (2000) also uses an ‘instability strip’ in a disk, in his case to explain the range of BEL widths. The radii at which the instability operates changes with \dot{m} , the accretion rate relative to the critical Eddington rate. Varying \dot{m} can explain the full range of BEL widths from $\sim 1000 \text{ km s}^{-1}$ for Narrow Line Seyfert 1s at high $\dot{m} \sim 1$, to the broadest lines at $\sim 20,000 \text{ km s}^{-1}$, lines, which occur the lowest \dot{m} consistent with the disk instability lying outside the minimum stable orbit and so still able to operate. LINERS may have \dot{m} below this value so that no BELR can form. Changing the radii having the instability will change the opening angle of the flow (§4.1). Some luminosity dependent changes (§6.2) may then reflect a more fundamental change in \dot{m} . Coupling Nicastro’s model with the model presented here seems to explain most of the emission and absorption line phenomena in AGN and quasars.

6.6. Radio Loud Quasars

BALs have been found, until recently, only in radio-quiet quasars (Stocke et al. 1992). This suggested quite strongly that the formation of BAL structures was intimately linked with a quasar’s radio properties. No such link is implied in the proposed structure. How can we reconcile this disjunction?

There are (at least) three options:

1. Observational bias: Goodrich (1997a) has shown that modest amounts of dust can reduce the observed fraction of BALs by a factor ~ 3 . So if radio-loud quasars are preferentially dustier than radio-quiets they would be relatively BAL-free. Such

quasars may be re-classified as ‘radio galaxies’ and so dropped from the samples (e.g. 3C22, Economou et al. 1995). A second effect may be ‘beaming bias’. Even a low frequency selected radio sample contains many quasars in which a beamed continuum dominates. These are seen pole-on and, in the proposed structure, would show no absorption. The FIRST survey has now found a substantial fraction of BALS (Becker et al. 1997, 1999, Gregg et al. 2000) and may be redressing these biases.

2. Jets destroy the BAL outflow: The presence of a relativistic jet will change the environment local to the flow. Cosmic rays or radiation may overionize the flow, reducing the radiation force. Alternatively the jet radiation or particle pressure may disrupt the outer part of the flow with a non-radial forces. Finally the harder continuum of a radio-loud quasar (Elvis et al. 1994) may be less effective at accelerating the outflow.
3. The outflow recollimates to form the jet: The most elegant solution is that the outflow re-collimates to form the jet. Jets are collimated and accelerated by means which are much debated (e.g. Cellotti and Blandford 2000). Even the scale on which these effects occur is not well determined. It is possible then that, e.g. magnetic fields, re-collimate the outflow near the point at which it would otherwise be accelerated radially to BAL velocities, and instead accelerates the flow toward the poles (figure 6.6) forming the jet. Kuncic (1999) and Vestergaard, Wilkes & Barthel (2000) make similar proposals. Junor et al. (1999) see a similar geometry in VLBI observations of M87: a 60° cone out to 100 Schwarzschild radii, where the jet then becomes collimated. If this suggestion is correct, then all radio-loud quasars (apart from those dominated by a beamed continuum) will show NALs (figure 6.6).

7. Conclusion

The structure proposed here is clearly ambitious. Yet, if we believe that quasars are a solvable problem, some coherent structure must be present. The present proposal, while in strong need of elaboration, draws together previously disparate areas of quasar research into a single simple scheme: the high and low ionization parts of the broad emission line region (BELR), the broad and narrow absorption line (BAL, NAL) regions, and the five Compton thick scattering regions can all be combined into the single funnel-shaped outflow. On large scales this outflow could produce the bi-conical narrow emission line regions and, with small geometric changes, several luminosity dependent effects can be understood. All of these features come about simply by requiring a geometry and kinematics constructed

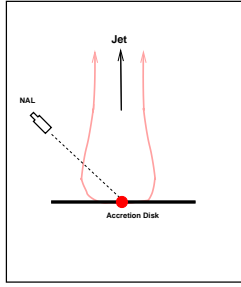


Fig. 8.— Geometry of a recollimated outflow in radio-loud quasars.

only to explain the two types of absorption lines. This unification gives the model a certain appeal.

Acknowledgments

This work has been made possible by the many fascinating and informative discussions I have had with my colleagues and friends at CfA and elsewhere, in particular with Ski Antonucci, Jill Bechtold, Nancy Brickhouse, Massimo Cappi, Bożena Czerny, Giuseppina (Pepi) Fabbiano, Fabrizio Fiore, Margarita Karovska, Andy Lawrence, Smita Mathur, Jonathan McDowell, Norm Murray, Fabrizio Nicastro, Brad Peterson, Richard Pogge, Aneta Siemiginowska, and Meg Urry. The 3-D renderings were kindly produced by Antoine Visonneau of the Center for Design Informatics at the Harvard School of Design using the 3D StudioMax software package. This work was supported in part by NASA contract NAS8-39073 (Chandra X-ray Center).

8. References

Almaini O., Boyle B. J., Griffiths R. E., Shanks T., Stewart G. C., & Georgantopoulos I., 1995, *MNRAS* **277**, L31.

Antonucci R., & Miller J.S., 1985, *Ap.J.* **621**.

Baldwin J.A., 1977, *Ap.J.*, **214** 679.

Baldwin J.A., 1997, in “Emission Lines in Active Galaxies: New Methods & Techniques” (IAU Colloquium 159), eds. B.M. Peterson, F.-Z. Chang & A.S. Wilson, *PAS Conf. Proc.*, **113** 85.

Becker R.H., Gregg M.D., Hook I.M., McMahon R.G., White R.I., & Helfand D.J., 1997, *Ap.J.*, **479**, L93.

Becker R.H., White R.L., Gregg M.D., Brotherton M., Laurent-Michelsen S., & Arav N., 2000, *Ap.J.*, submitted.

Begelman M.C., Mc Kee C.F. & Shields G.A., 1983, *Ap.J.*, **271** 70.

Berriman G., Schmidt G.D., West S.C., & Stockman H.S. 1990, *Ap.J.S.*, **74**, 869.

Beloborodov A.M. & Poutanen J., 1999, *Ap.J.Letters*, **517**, L77.

Binette L., 1998, *MNRAS*, **294**, L47

Bottorf M.C., Korista K.T., Shlosman I. & Blandford R.D., 1997, *Ap.J.*, **479**, 200

Bromley B.C., Miller W.A. & Pariev V.I., 1998, *Nature* **391**, 54.

Campbell C.G., 1999, *MNRAS*, **310**, 1175

Capetti, A. Macchetto, F.D., & Lattanzi, M.G., 1997, *Ap.J.*, **476**, L67.

Capetti, A., Axon, D.J., Macchetto, F.D., Sparks, W.B., & Boksenberg, A. 1996, *Ap.J.*, **466**, 166.

Cassidy I. & Raine D.J., 1993, *MNRAS*, **260** 385.

Cassidy I. & Raine D.J., 1996, *A&A* **310**, 44.

Cellotti A. and Blandford R.D. 2000, in “Black Holes in Binaries and Galactic Nuclei”, eds. L. Kaper, E.P.J. van den Heuvel, P.A. woodt [springer-Verleg].

Chiang J., Reynolds C.S., Blaes O.M., Nowak M.A., Murray N., Madejski G., Marshall H.L. & Magdziarz P., 2000, *Ap.J.*, **528**, 292

Clavel J. Wamsteker W. & Glass I.S., 1989, *Ap.J.*, **337**, 236

Cohen M.H., Ogle P.M., Tran H.D., Vermuelen R.C., Miller J.S., Goodrich R.W. & Martel A.R., 1995, *ApJ* **448**, L77.

Collin-Souffrin S., Dyson J.E., McDowell J.C. & Perry J.J., 1988, *MNRAS* **232**, 539.

Comastri A., Setti G., Zamorani G. & Hasinger G., 1995, *A&A* **296**, 1.

Costantini E., et al., 2000, *ApJ*, submitted

Crenshaw D.M. & Kraemer S.B., 2000, *Ap.J.Letters*, **532**, L101.

Crenshaw D.M., Kraemer S.B., Boggess A., Marran S.P., Mushotzky, R.F., & Wu C.-C., 1999, *Ap.J.*, **516**, 750.

Crenshaw D.M. and Kraemer S.B. 1999, *Ap.J.*, **521**, 572.

deKool M., 1997, “Mass Ejection from AGN”, eds. N. Arav, I. Shlosman & R.J. Weymann, ASP Conf. Series, 128, 233.

Done C., Madejski G.M. & Źycki P.T., 2000, [astro-ph/0002023](http://arxiv.org/abs/astro-ph/0002023)

Economou F., Lawrence A., Ward M.J. & Blanco P.R., 1995, *MNRAS*, **272**, L5

Edelson R.A., Malkan M.A., Rieke G.F., 1987, *Ap.J.* **321**, 233.

Elvis M., et al. 1994, *Ap.J.S.*, **95**, 1.

Emmering R.T., Blandford R.D. & Shlosman I., 1992, *Ap.J.*, **385**, 460

Espey B.R. & Andreadis S.J., 1999, “Quasars and Cosmology”, ASP Conf. Series, **162**, 351.

Fabian A.C., et al. 1994, *PASJ*, **46**, L59.

Fabian A.C., et al. 1995, *MNRAS* **277** L11.

Feldmeier A., Norman C., Pauldrach A., Owocki S., Puls J. & Kaper L., 1997, “Mass Ejection from AGN”, eds. N. Arav, I. Shlosman & R.J. Weymann, ASP Conf. Series, **128**, 258.

Ferland G.J., Korista K.T. & Peterson B.M., 1990, *Ap.J.* **363**, L21.

Ferland G.J., Peterson B.M., Horne K., Welsh W.F. & Nahar S.N., 1992, *Ap.J.* **387**, 95.

Gallagher S.C., Brandt W.N., Sambruna R.M., Mathur S. & Yamasaki, 1999, *Ap.J.*, in press.

Georgantopoulos I., Papadakis I., Warwick R.S., Smith D.A., Stewart G.C. & Griffiths R.G., 1999, *MNRAS* submitted (astro-ph/9903083).

George I.M. & Fabian A.C., 1991, *MNRAS* **249**, 352.

George I.M., Turner T.J. & Netzer H., 1995, *Ap.J.L.* **438**, L67.

Goad R.W. & Koratkar A.P., 1998, *Ap.J.* **495** 718.

Goad R.W., Koratkar A.P., Axon A.J., Korista K.T. & O'Brien P.T., 1999, *Ap.J.(Letters)*, **512** L95.

Goodrich R.W. & Miller J.S., 1994, *Ap.J.* **434**, 82.

Goodrich R.W. & Miller J.S., 1995, *Ap.JL* **448**, L73.

Goodrich R.W., 1997a, “Mass Ejection from AGN”, edS. N. Arav, I. Shlosman & R.J. Weymann, ASP Conf. Series, **128**, 94.

Goodrich R.W., 1997b, *Ap.J.*, **474**, 606.

Gregg M., et al. 2000, in preparation.

Habing H.J., 1996, *A & A Rev.*, **7**, 97

Halpern J.P. & Moran E., 1998, *Ap.J.*, **494**, 194.

Hamann F., Korista K.T. & Morris S.L., 1993, *Ap.J.* **415**, 541.

Hamann F., Shields J.C., Ferland G.J. & Korista K., 1995a, *Ap.J.* **454**, 688.

Hamann F., Zuo L & Tytler D., 1995b, *Ap.J.L* **444**, L69.

Hamman F., 1998, *Ap.J.*, **500**, 798.

Ho L.C., 1998, in ‘Observational Evidence for Black Holes in the Universe’, ed. S.K. Chakrabati [Dordrecht:Kluwer], p.

Huchra J.P. & Burg R., 1992, *Ap.J.* **393**, 90.

Impey C.D., Malkan M.A., Webb W. & Petry C.E., 1995, *Ap.J* **440**, 80.

Iwasawa K. & Taniguchi Y., 1993, *Ap.J.L* **413**, L15.

Iwasawa K., Fabian A.C., Young A.J., Inoue, H., & Matsumoto C., 1999, *MNRAS*, **306**, L19.

Junor, W., Biretta, J.A., & Livio, M. 1999, *Nature*, **401**, 891.

Kaastra J.S., Roos N. & Mewe R., 1995, *A&A*, **300**, 25.

Kay L.E., 1994, *Ap.J.* **430**, 196.

Komossa S., 1999, in “Structure and Kinematics of Quasar Broad Line Regions”, ASP Conference Series, 175. eds. C. M. Gaskell, W.N. Brandt, M. Dietrich, D. Dultzin-Hacyan & M. Eracleous, p.365

Koratkar A., Antonucci R.R.J., Goodrich R.W., Bushouse H. & Kinney A.L., 1995, *Ap.J.* **450**, 501.

Korista, K.T., et al. 1995, *Ap.J.S.*, **97**, 285.

Krolik J.H. & Kriss G.A., 1995, *Ap.J.* **447**, 512.

Krolik J.H., 1999, “Active Galactic Nuclei” [Princeton: Princeton University Press].

Krolik J.H., McKee C. & Tarter B., 1981, *Ap.J.* **249** 422.

Kuncic Z. 1999, *PASP*, **111**, 954.

Kurpiewski A., Kurasczkiewicz J. & Czerny B., 1997, *MNRAS* **285**, 725.

Lawrence A. and Elvis M., 1982, *Ap.J.* **256**, 410.

Lee L.W. & Turnshek D.A., 1995, *Ap.J.(Letters)*, **453**, L61

Lightman A.P. & White T.R., 1988, *Ap.J.* **335**, 57.

Madejski G.M., Źycki P., Done C., Valinin A., Blanco P., Rothschild R. & Turek B., 2000, *Ap.J.Letters* in press. [astro-ph/0002063](#)

Maiolino R. & Rieke G.H., 1995, *Ap.J.* **454**, 95.

Maoz D., Edelson R. & Nandra K., 1999, [astro-ph/9910023](#)

Malkan M.A., Gorjian V., Tam R., 1998, *Ap.J.(Supp.)*, **117**, 25.

Marshall H.L., et al. 1997, *Ap.J.*, **479**, 222.

Mathur S., Elvis M. & Singh K.P., 1996, *Ap.J.* **455**, L9.

Mathur S., Elvis M. & Wilkes B.J., 1995, *Ap.J.* **452**, 230.

Mathur S., Elvis M. & Wilkes B.J., 1999, *Ap.J.*, **519**, 605.

Mathur S., Wilkes B.J. & Elvis M., 1998, *Ap.J.(Letters)*, **503**, L23.

Mathur S., et al., 2000, *Ap.J.(Letters)*, in press.

Matt G., Fabian A.C. & Ross R., 1991, *MNRAS* **262**, 179.

Matthews W.G., 1974, *Ap.J.* **189**, 23.

Matthews W.G., 1986, *Ap.J.* **305**, 187.

McHardy I. et al. 1995, *MNRAS* **273**, 549.

Miller J.S. & Goodrich R.W., 1990, *Ap.J.* **355**, 456.

Miller J.S., Goodrich R.W. & Mathews W., 1991, *Ap.J.* **378**, 47.

Murray N. & Chiang J., 1995, *Ap.J.L* **454**, L105.

Murray N. & Chiang J., 1998, *Ap.J.*, **494**, 125.

Murray N., Chiang J., Grossman S.A. & Voit G.M., 1995 *Ap.J.* **451**, 498.

Nandra K., George I.M., Mushotzky R.F., Turner T.J., & Yaqoob T., 1997a, *Ap.J.*, **477** 602.

Nandra K., George I.M., Mushotzky R.F., Turner T.J., Yaqoob T., 1997b, *Ap.J.*, **488** L91.

Netzer H., 1993, *Ap.J.* **473**, 781.

Nicastro F., 2000, *Ap.J.Letters*, 530, L65

Nicastro F., Fiore F., Perola G.C. & Elvis M., 1999, *Ap.J.* **512**, 184.

Nicastro F., et al, 2000, *Ap.J.*, in press. [astro-ph/001201](http://arxiv.org/abs/astro-ph/001201)

Ogle P.M., 1997, “Mass Ejection from AGN”, eds. N. Arav, I. Shlosman & R.J. Weymann, ASP Conf. Series, **128**, 78.

Ogle P.M., 1998, PhD thesis, California Institute of Technology.

Osmer P.S., & Shields J.C., 1999, “Quasars and Cosmology”, ASP Conf. Series, **162**, 235.

Osterbrock D.E., 1989, “Astrophysics of Gaseous Nebulae and Active Galactic Nuclei” [Mill Valley: Univ. Science Books].

Peterson B.M., 1993, *PASP*, **105**, 247

Peterson B.M., 1997, ‘An Introduction to Active Galactic Nuclei’ [Cambridge:CUP].

Peterson B.M. & Wandel A., 1999, *Ap.J.(Letters)*, 521, L95

Peterson B.M. & Wandel A., 2000, in preparation

Pier E.A & Krolik J.H., 1992, *Ap.J.(Letters)* **399**, L23.

Piro L., Yamauchi M. & Matsuoka M., 1990, *Ap.J.* **360**, L35.

Porquet D., Dumont A.-M., Collin S. & Mouchet M., 1999, *A&A*, **341** 58.

Pounds K.A., Nandra K., Stewart G.C., George I.M. & Fabian, A., 1990, *Nature*, **344**, 132.

Proga D., Stone J.M., & Drew J.E. 1998, *MNRAS*, **296**, L6.

Proga D., Stone J.M., & Drew J.E. 1999, *MNRAS*, **310**, 476.

Proga D., Stone J.M., & Kallman T.R. 2000, [astro-ph/0005315](#)

Reynolds C.S., 1997, *MNRAS* **286**, 513.

Rudge C.M. & Raine D.J., 1998, *MNRAS* **297**, L1.

Rush B., Malkan M.A. & Spinoglio L., 1993, *Ap.J.S* **89**, 1.

Salpeter E.E., 1974, *Ap.J.*, **193**, 585

Schild R.E., 1996, *Ap.J.*, **464**, 125

Schinnerer E., Eckart A., Tacconi L.J., Genzel R. & Downes D., *ApJ*, in press
([astro-ph/9911488](#))

Schmidt G.D. & Hines D.C., 1999, *Ap.J.*, **512**, 125.

Shields J.C., 1994, “Reverberation mapping of the broad-line region in active galactic Nuclei”, eds. Goodhalekar, P.M. Horne, K. and Petterson, B.M., ASP Conference Series 69, 293.

Shields J.C., Ferland G.J. & Peterson B.M., 1995, *Ap.J.* **441**, 507.

Shull M.J. & Sachs E.R., 1993, *Ap.J.* **416**, 536.

Simcoe J.A., McLeod K.K., Schachter, J. & Elvis M., 1998, *Ap.J.*, **489**, 615.

Stocke, J.J., Morris. S.L., Weymann, R.J. & Foltz, C.B., 1992, *Ap.J.*, **396**, 487.

Tadhunter C. & Tsvetanov Z., 1989, *Nature* **341**, 422.

Tanaka Y. et al. 1995, *Nature*, **375**, 649.

Telfer R.C., Kriss G.A., Zheng W., Davidsen A.F. & Green R.F., 1998, *Ap.J.*, **509**, 132.

Turner T.J., Nandra K., George I.M., Fabian A.C. & Pounds K.A., 1993, *Ap.J.* **419**, 127.

Turnshek D.A., 1988 “QSO Absorption Lines: Probing the Universe”, eds. J.C. Blades, D.A. Turnshek, C.A. Norman [Cambridge:CUP], p. 17.

Turnshek D.A., Kopko M., Monier E., Noll D., Espey B.R. & Weymann R.J., 1996, *Ap.J.* **463**, 110.

Vestergaard M., 2000, *PhD Thesis*, Niels Bohr Institute for Astronomy, Physics & Geophysics, Copenhagen University

Vignali et al., 2000, *ApJ*, submitted

Vestergaard M., Wilkes B.J. & Barthel P., 2000, *Ap.J. (Letters)*, submitted

Wang J.X., Zhou Y.Y., Xu H.G., & Wang T.G., 1999, *Ap.J. (Letters)*, **516**, L65.

Weymann R.J., Morris S.L., Foltz C.B. & Hewett P.C., 1991 *Ap.J.* **373**, 23.

Wilkes B.J., 1984, *MNRAS* **207**, 73.

Williams R.J.R., 2000, *MNRAS*, submitted

Yaqoob T., Serlemitsos P.J., Turner T.J., George I.M. & Nandra K., 1996, *Ap.J.* **470**, L27.

Young S., Corbett E.A., Giannuzzo M.E., Hough J.H., Robinson A., Bailey J.A. & Axon D.J., 1999, *MNRAS*, **303**, 227.

Życki P.T. & Czerny B., 1994, *MNRAS* **266** 653.